 Printed in China Communications in Theoretical Physics

Commun. Theor. Phys. **77** (2025) 085404 (7pp) https://doi.org/10.1088/1572-9494/adb5f7
CSTR: 32041.14.CTP.adb5f7

QCD axion bubbles in the presence of ALP resonant conversion

Hai-Jun Li

Key Laboratory of Theoretical Physics, Institute of Theoretical Physics, Chinese Academy of Sciences, Beijing 100190, China
Center for Advanced Quantum Studies, Department of Physics, Beijing Normal University, Beijing 100875, China

E-mail: lihaijun@itp.ac.cn

Received 28 October 2024, revised 14 December 2024
Accepted for publication 5 February 2025
Published 28 April 2025

Abstract

The QCD axion bubbles can form due to an explicit breaking of the Peccei–Quinn symmetry in the early Universe. In this paper, we investigate the modified formation of a QCD axion bubble in the presence of an axionlike particle (ALP), considering its resonant conversion to a QCD axion. We consider a general scenario where the QCD axion mixes with ALP before the QCD phase transition. In this scenario, the energy density of the ALP can be adiabatically transferred to the QCD axion at a temperature T_R, resulting in the suppression of the cosmic background temperature T_B at which the energy density of the QCD axion equals that of the radiation. The QCD axion bubbles form when the QCD axions arise during the QCD phase transition. Finally, we briefly discuss the impact of the formation of QCD axion bubbles on the formation of primordial black holes.

Keywords: axion, axionlike particle, primordial black hole

(Some figures may appear in colour only in the online journal)

1. Introduction

The strong CP problem in the Standard Model (SM) is a long-standing problem and can be solved by the Peccei-Quinn (PQ) mechanism with a spontaneously broken $U(1)$ PQ symmetry [1, 2]. The PQ mechanism predicted a light pseudo Nambu-Goldstone (NG) boson, axion (also called the QCD axion) [3, 4], which acquires a tiny mass from the QCD non-perturbative effects [5, 6]. When the potential of the QCD axion is generated by the QCD instanton, the axion is stable at the minimum value of CP conservation, which solves the strong CP problem. The QCD axion is the potential cold dark matter (DM) candidate if non-thermally produced in the early Universe through the misalignment mechanism [7–9]. The QCD axion is massless at high temperatures. As the cosmic temperature decreases, it acquires a non-zero mass during the QCD phase transition and starts to oscillate when its mass becomes comparable to the Hubble parameter, which explains the observed DM abundance. See e.g. [10–12] for recent reviews.

The PQ symmetry is supposedly broken before or during inflation. In this case, the QCD axion is massless during inflation and acquires quantum fluctuations. To suppress the isocurvature perturbations, a feasible method is considering an explicit PQ symmetry breaking [13–16]. The PQ symmetry is an approximate global symmetry and can be strongly broken in the early Universe with the multiple vacua [17–23]. The QCD axion bubbles [24] can form due to this explicit PQ symmetry breaking. In this case, axion acquires a light mass and oscillates when this mass is greater than the Hubble parameter. Note that the explicit PQ symmetry breaking potential for the axion will disappear before the QCD phase transition. Therefore, the final QCD axion abundance can also be calculated through the misalignment mechanism. However, the initial misalignment angle is determined by the explicit PQ symmetry breaking, which can be split into different values. If the axion initial value is smaller than a critical value, the axion is stabilized near the origin. On the contrary, the axion will be stabilized at another minimum if the axion initial value is larger than the critical value. During the QCD

phase transition, the QCD axions start to oscillate near the origin and another large value. The former case can account for the cold DM abundance, while the latter can form the high axion density region, which is called the QCD axion bubble. The concept of QCD axion bubbles was first proposed in [24], which is similar to the baryon bubbles in the inhomogeneous Affleck-Dine baryogenesis [25, 26]. Additionally, they also investigated the formations of the primordial black holes (PBHs) and axion miniclusters from the QCD axion bubbles.

In this paper, we investigate the modified QCD axion bubble formation in the presence of the axionlike particle (ALP) to QCD axion resonant conversion. We introduce a general case that the QCD axion mixes with ALP before the QCD phase transition. In this case, the ALP to QCD axion resonant conversion is considered to take place at the temperature T_R, and the ALP energy density can be adiabatically transferred to the QCD axion. We find that this will lead to the suppression of the cosmic background temperature T_B in which the QCD axion energy density is equal to the radiation energy density. The QCD axion bubbles are formed when the QCD axions arise during the QCD phase transition. Finally, we briefly discuss this impact on the PBHs formation in the QCD axion bubbles scenario, leading to the enhancement of the minimum PBH mass.

The rest of this paper is organized as follows. In section 2, we briefly review the QCD axion DM and the misalignment mechanism. In section 3, we investigate the effect on QCD axion bubble formation in the presence of the ALP resonant conversion, and also the impact on PBHs formation in the QCD axion bubbles scenario. Finally, the conclusion is given in section 4.

2. QCD axion and misalignment mechanism

Here we briefly review the QCD axion DM and the misalignment mechanism. The QCD axion is a pseudo NG boson with a spontaneously broken $U(1)$ PQ symmetry. It couples to gluons with the following effective Lagrangian

$$\mathcal{L}_{agg} = -\frac{\alpha_s}{8\pi}\frac{\phi}{f_a}G^{a\,\mu\nu}\tilde{G}^a_{\mu\nu}, \tag{1}$$

where α_s is the strong fine structure constant, ϕ is the QCD axion field, $f_a = v_a/N_{\rm DW}$ is the axion decay constant, v_a is the spontaneous breaking scale of the PQ symmetry, $N_{\rm DW}$ is the number of the domain wall, $G^{a\,\mu\nu}$ and $\tilde{G}^a_{\mu\nu}$ are the gluon field strength tensor and dual tensor, respectively. The resulting effective potential of the QCD axion is given by

$$V_{\rm QCD}(\phi) = m_a^2(T)f_a^2\left[1-\cos\left(\frac{\phi}{f_a}\right)\right], \tag{2}$$

where $m_a(T)$ is the temperature-dependent QCD axion mass for $T \gtrsim T_{\rm QCD}$ ($\sim 150\,$MeV) [27]

$$m_a(T) \simeq m_{a,0}\left(\frac{T}{T_{\rm QCD}}\right)^{-4.08}, \tag{3}$$

with the zero-temperature axion mass [28]

$$m_{a,0} \simeq 5.70(7)\,\mu{\rm eV}\left(\frac{f_a}{10^{12}\,{\rm GeV}}\right)^{-1}. \tag{4}$$

In the misalignment mechanism [7–9], as the cosmic temperature decreases the QCD axion starts to oscillate when its mass $m_a(T)$ becomes comparable to the Hubble parameter $H(T)$

$$3H(T_a) = m_a(T_a), \tag{5}$$

then we have the oscillation temperature

$$T_a \simeq 0.96\,{\rm GeV}\left(\frac{g_*(T_a)}{61.75}\right)^{-0.082}\left(\frac{f_a}{10^{12}\,{\rm GeV}}\right)^{-0.16}, \tag{6}$$

where $g_*(T)$ is the number of effective degrees of freedom of the energy density. The QCD axion number density at T_a is given by

$$n_a(T_a) = \frac{1}{2}m_a(T_a)f_a^2\,\langle\theta_i^2 f(\theta_i)\rangle\,\chi, \tag{7}$$

where θ_i is the initial misalignment angle, $\chi \simeq 1.44$ is a numerical factor [29], and $f(\theta_i)$ is the anharmonic factor

$$f(\theta_i) \simeq \left[\ln\left(\frac{e}{1-\theta_i^2/\pi^2}\right)\right]^{1.16}, \tag{8}$$

which is taken as $f(\theta_i) \simeq 1$ for $|\theta_i| \ll \pi$ [30, 31]. The present axion energy density $\rho_a(T_0) = m_{a,0}n_a(T_0)$ is

$$\rho_a(T_0) = \frac{m_{a,0}m_a(T_a)s(T_0)}{2s(T_a)}f_a^2\,\langle\theta_i^2 f(\theta_i)\rangle\,\chi, \tag{9}$$

where $s(T) = 2\pi^2 g_{*s}(T)T^3/45$ is the entropy density, $g_{*s}(T)$ is the number of effective degrees of freedom of the entropy density, and T_0 is the present CMB temperature. Then we have the current QCD axion abundance $\Omega_a h^2 = \rho_a(T_0)/\rho_c h^2$ as

$$\Omega_a h^2 \simeq 0.14\left(\frac{g_{*s}(T_0)}{3.94}\right)\left(\frac{g_*(T_a)}{61.75}\right)^{-0.42} \times \left(\frac{f_a}{10^{12}\,GeV}\right)^{1.16}\langle\theta_i^2 f(\theta_i)\rangle, \tag{10}$$

where $\rho_c = 3H_0^2M_{\rm Pl}^2$ is the critical energy density, $M_{\rm Pl} \simeq 2.44 \times 10^{18}\,GeV$ is the reduced Planck mass, and $h \simeq 0.68$ is the reduced Hubble constant. In order to explain the observed cold DM abundance, $\Omega_{\rm DM}h^2 \simeq 0.12$ [32], we derive the initial misalignment angle

$$\theta_i \simeq 0.87\left(\frac{g_{*s}(T_0)}{3.94}\right)^{-1/2}\left(\frac{g_*(T_a)}{61.75}\right)^{0.21} \times \left(\frac{f_a}{10^{12}\,GeV}\right)^{-0.58}, \tag{11}$$

which is valid for $f_a \lesssim 10^{17}\,GeV$.

3. QCD axion bubbles in the presence of ALP resonant conversion

In this section, we investigate the effect on QCD axion bubble formation in the presence of the ALP to QCD axion resonant

conversion, and also the impact on PBHs formation from the QCD axion bubbles.

3.1. QCD axion bubbles

The QCD axion bubbles can form due to an explicit PQ symmetry breaking in the early Universe and are formed during the QCD phase transition. There are many scenarios for this explicit PQ symmetry breaking, such as the Witten effect of monopoles in hidden sectors [33–35], a larger scale of the spontaneous PQ symmetry breaking with the higher dimensional term [36–39], the hidden non-Abelian gauge interactions [15], and a stronger QCD with the large Higgs field expectation value [14, 40]. In [24], they considered the Witten effect as an example of the explicit PQ symmetry breaking to form the QCD axion bubbles. Considering a large axion decay constant $f_a \sim \mathcal{O}(10^{16} - 10^{17})\,GeV$ and the axion is stabilized at the potential minima with

$$\phi^0_{\rm min} \simeq 0, \quad \phi^1_{\rm min} \simeq \pi f_a, \quad \cdots, \tag{12}$$

which corresponds to the effective initial misalignment angle $\theta_{i,n}$ with

$$\theta_{i,0} = 0 - \theta_i, \quad \theta_{i,1} = \pi - \theta_i, \quad \cdots. \tag{13}$$

When the QCD axion $V_{\rm QCD}(\phi)$ arises during the QCD phase transition, the state $\phi^0_{\rm min}$ with the effective initial angle $\theta_{i,0}$ explains the cold DM abundance, corresponding to a small initial misalignment angle

$$\theta_i \simeq 4.29 \times 10^{-3}\left(\frac{g_{*s}(T_0)}{3.94}\right)^{-1/2}\left(\frac{g_*(T_a)}{61.75}\right)^{0.21} \times \left(\frac{f_a}{10^{16}\,GeV}\right)^{-0.58}. \tag{14}$$

On the other hand, if the initial value of axion is larger than a critical value $\phi_{\rm crit}$, the axion will settle down into the minimum $\phi^1_{\rm min}$ with the initial angle $\theta_{i,1}$. In this case, since the large initial misalignment angle π, the local axion density at the minimum $\phi^1_{\rm min}$ becomes much higher than that at $\phi^0_{\rm min}$, which forms the high-density QCD axion bubbles. When the axion dominates the radiation in the bubbles, i. *e*., the axion energy density is equal to the radiation energy density, we can define the cosmic background temperature, T_B. The local axion energy density in the bubbles at T_B is given by

$$\rho_{a,B} = \frac{m_{a,0} m_a(T_a) s(T_B)}{2 s(T_a)} f_a^2 \langle \theta^2_{i,1} f(\theta_{i,1})\rangle \chi, \tag{15}$$

and the radiation energy density is defined as

$$\rho_{R,B} = \frac{\pi^2}{30} g_*(T_B) T_B^4. \tag{16}$$

Considering $\rho_{a,B} = \rho_{R,B}$ and the effective initial angle $\theta_{i,1} = \pi - \theta_i$, we have the temperature

$$T_B \simeq 2.13 \times 10^{-2}\,{\rm MeV} \times \left(\frac{g_*(T_a)}{61.75}\right)^{-0.42} \times \left(\frac{f_a}{10^{16}\,GeV}\right)^{1.16} \langle \theta^2_{i,1} f(\theta_{i,1})\rangle \chi. \tag{17}$$

Substituting equation (14) into equation (17), we can derive $T_B \simeq 2.84\,{\rm MeV}$ for $f_a \sim \mathcal{O}(10^{16})\,GeV$.

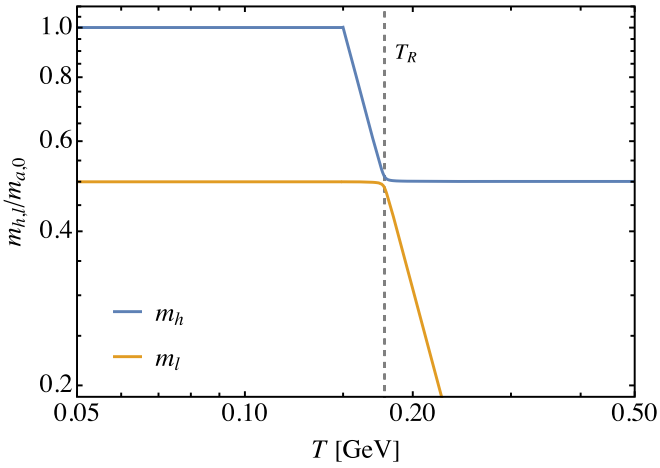

Figure 1. Illustration of the ALP to QCD axion resonant conversion at the temperature T_R. The solid lines distinctly represent the normalized temperature-dependent mass eigenvalues, where $m_h(T)$ and $m_l(T)$ denote the heavy and light mass eigenvalues, respectively, as they evolve with temperature. Notice that the cosmic temperature decreases from right to left in the plot. This graphical representation provides insight into the dynamic interplay between the ALP and QCD axion masses during the resonant conversion. Here we set $f_a = 10^{16}\,GeV$, $f_a/f_A = 20$, and $m_{a,0}/m_A = 2$.

3.2. ALP to QCD axion resonant conversion

In the following, we investigate the effect in the presence of the ALP to QCD axion resonant conversion. We consider a general case that the QCD axion mixes with ALP with the mixing potential [41, 42]

$$V_{\rm mix}(\phi, \varphi) = m_A^2 f_A^2\left[1 - \cos\left(\frac{\phi}{f_a} + \frac{\varphi}{f_A} + \delta\right)\right] + m_a^2(T) f_a^2\left[1 - \cos\left(\frac{\phi}{f_a}\right)\right], \tag{18}$$

where φ is the ALP field, m_A and f_A are the ALP mass and the decay constant, respectively, and δ is the CP phase. For simplicity, in this context, we assume a temperature-independent ALP mass[1] and take the CP phase δ to be zero.[2] The mass mixing matrix is given by

$$\mathbf{M}^2 = \begin{pmatrix} m_a^2(T) + \frac{m_A^2 f_A^2}{f_a^2} & \frac{m_A^2 f_A}{f_a} \\ \frac{m_A^2 f_A}{f_a} & m_A^2 \end{pmatrix}, \tag{19}$$

then we can derive the heavy and light mass eigenvalues $m_{h,l}(T)$. See figure 1 for the illustration of the normalized mass eigenvalues as functions of the cosmic temperature T. Here we consider the conditions under which the ALP to QCD

[1] Given that ALP does not have a specific model detailing its mass variation with temperature, unlike the QCD axion, we have chosen, for the sake of simplicity and in accordance with prevalent practices in the literature, to adopt a constant-temperature mass model for ALP in our analysis.

[2] This can be regarded as equivalent to requiring an independent solution to the strong CP problem. Since this assignment has no bearing on the evolution of the two axion fields during their mixing, it consequently leaves the axion energy density in our scenario unaltered.

axion resonant conversion can take place:

$$\frac{f_a}{f_A} > 1, \quad \frac{m_{a,0}}{m_A} > 1. \tag{20}$$

In this case, the resonant conversion occurs at the temperature T_R, which is given by

$$m_a(T_R) \simeq m_A. \tag{21}$$

At the temperature $T > T_R$, the light mass eigenstate m_l is associated with the QCD axion, whereas below T_R, it is the heavy mass eigenstate m_h that comprises the QCD axion. Conversely, at the temperature above T_R, the heavy mass eigenstate m_h pertains to the ALP, whereas at the temperature below T_R, it is the light mass eigenstate m_l that forms the ALP. The axion energy transition at T_R is considered to be adiabatic, which can be roughly satisfied when

$$T_a \gg T_R, \tag{22}$$

where T_a is the QCD axion oscillation temperature.

To obtain the energy density of the QCD axion at the temperature $T_B^{'}$, we should begin with the ALP field at high temperatures. Its initial energy density at the oscillation temperature $T_{i,A}$ is given by

$$\rho_{A,i} = \frac{1}{2} m_A^2 f_A^2 \theta_{i,A}^2, \tag{23}$$

where $\theta_{i,A}$ is the initial misalignment angle of the ALP. At $T_R < T < T_{i,A}$, the ALP energy density is adiabatic invariant. Using $N_A \equiv \rho_A a^3/m_A$, where a is the scale factor, we have the ALP energy density at the temperature T_R as

$$\rho_{A,R} = \frac{1}{2} m_A^2 f_A^2 \theta_{i,A}^2 \left(\frac{a_{i,A}}{a_R}\right)^3, \tag{24}$$

where $a_{i,A}$ and a_R correspond to the scale factors at $T_{i,A}$ and T_R, respectively. At T_R, the ALP energy density $\rho_{A,R}$ is adiabatically transferred to the QCD axion $\rho_{a,R}$. Then at $T_B^{'} < T < T_R$, the adiabatic approximation is valid again with $N_a \equiv \rho_a a^3/m_a$, and we have the QCD axion energy density at $T_B^{'}$ as

$$\rho_{a,B}^{'} = \frac{1}{2} m_{a,0} m_A f_A^2 \theta_{i,A}^2 \left(\frac{a_{i,A}}{a_B^{'}}\right)^3, \tag{25}$$

where $a_B^{'}$ is the scale factor at $T_B^{'}$. Note that $T_B^{'}$ is given by $\rho_{a,B}^{'} = \rho_{R,B}^{'}$. Now compared with the no ALP resonant conversion case

$$\rho_{a,B} = \frac{1}{2} m_{a,0} m_{a,i} f_a^2 \theta_{i,1}^2 \left(\frac{a_{i,a}}{a_B}\right)^3, \tag{26}$$

we find that the temperature T_B can be suppressed as

$$\frac{T_B^{'}}{T_B} \simeq \sqrt[4]{\frac{m_A f_A^2 \theta_{i,A}^2}{m_{a,i} f_a^2 \theta_{i,1}^2} \left(\frac{a_{i,A} a_B}{a_{i,a} a_B^{'}}\right)^3} = \frac{m_{a,i}^{1/2} f_A^2 \theta_{i,A}^2}{\pi^2 m_A^{1/2} f_a^2}, \tag{27}$$

where $m_{a,i} \equiv m_a(T_a)$. Note that $a(T) \propto \sqrt{t} \propto 1/T \propto 1/\sqrt{H}$, $a_i(T) \propto 1/\sqrt{H} \propto 1/\sqrt{m_i}$, and m_i corresponds to the axion mass at the oscillation temperature that given by $3H = m_i$. In figure 2, we show the distributions of this factor across the $\{\log(f_a/f_A), \log(m_{a,i}/m_A)\}$ plane with $\theta_{i,A} = \pi$ and $\pi/2$, respectively. We find that within the defined range of the parameter space we are examining, the temperature T_B undergoes a notable suppression. One can further calculate the present QCD axion energy density in this manner to explain the abundance of cold DM, but this is not the focus of the current context and therefore is not presented here. For further details, please refer to [41, 42].

3.3. Primordial black holes

In this subsection, we provide a concise overview of the formation of PBHs from the QCD axion bubbles. PBHs, which can arise from significant density perturbations in the early Universe, are also compelling candidates for DM [43–47]. At the time of their formation t_f, the initial mass of a PBH is described by the formula $M_{\rm PBH} = 4\pi\gamma\rho_R/(3H_f^3)$ [48], where $\gamma \simeq 0.2$ is the gravitational collapse factor [49], ρ_R represents the radiation energy density, and H_f is the Hubble parameter at t_f. Subsequently, we derive the PBH mass at the formation time as follows:

$$\frac{M_{\rm PBH}}{M_\odot} \simeq 0.03 \times \left(\frac{\gamma}{0.2}\right)\left(\frac{g_*(T_f)}{10.75}\right)^{-1/2} \times \left(\frac{T_f}{1\,GeV}\right)^{-2}, \tag{28}$$

where T_f corresponds to the temperature at t_f, and $M_\odot$ denotes the solar mass. This equation allows us to estimate the PBH mass based on the relevant physical parameters.

In the context of the QCD axion bubbles scenario [24], PBHs form when axions dominate the radiation inside the bubbles, i. *e.* , when the temperature T_f is less than or equal to the cosmic background temperature T_B, and the bubble size exceeds the horizon size.[3] When these bubbles enter the horizon, the local energy density within them significantly surpasses the background radiation density. Given that the mass of a PBH resulting from bubble collapse cannot exceed the background horizon mass by much [50, 51], it is assumed that the PBH mass in the axion bubbles scenario is equivalent to the horizon mass of the background radiation, even when $T_f < T_B$. By substituting equation (17) into equation (28), we derive the minimum PBH mass

$$\frac{M_{\rm PBH}^{\rm min}}{M_\odot} \simeq 6.58 \times 10^7 \left(\frac{\gamma}{0.2}\right)\left(\frac{g_*(T_f)}{10.75}\right)^{-1/2} \times \left(\frac{g_*(T_a)}{61.75}\right)^{0.84}\left(\frac{f_a}{10^{16}\,GeV}\right)^{-2.33} \times \left(\langle\theta_{i,1}^2 f(\theta_{i,1})\rangle\,\chi\right)^{-2}. \tag{29}$$

For $f_a \sim \mathcal{O}(10^{16})\,GeV$, the minimum PBH mass is approximately $M_{\rm PBH}^{\rm min} \simeq 3.71 \times 10^3 M_\odot$. When considering the impact of resonant conversion from ALP to QCD axion, we find that

[3] Note that the fluctuation of ALPs may also have an impact on the production of PBHs in the early Universe. However, since our focus here is on PBHs generated by modified QCD axion bubbles, we have not considered this effect separately. Further discussion on this effect may be included in future work.

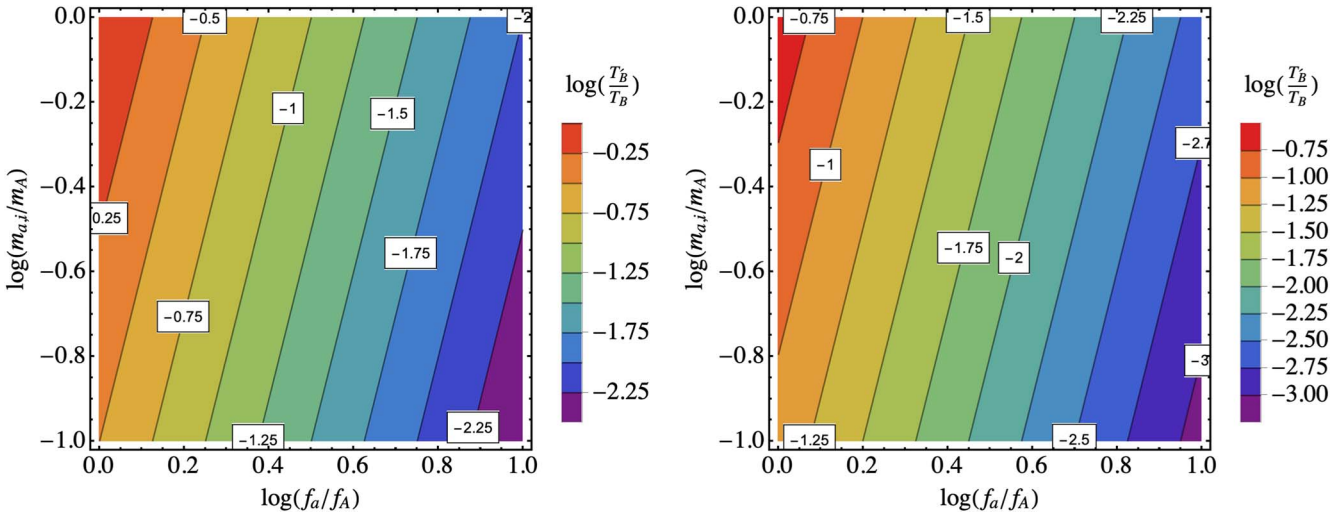

Figure 2. Variations in the temperature ratio $T_B^{'}/T_B$, defined by equation (27), across the $\{\log(f_a/f_A), \log(m_{a,i}/m_A)\}$ parameter space. Left panel: displays the distribution when a specific set of parameters $\theta_{i,A} = \pi$ is applied. Right panel: shows the distribution for an alternative set of parameters $\theta_{i,A} = \pi/2$. These panels not only illustrate how the temperature ratio distribution varies within the given parameter range but also highlight the potential for significant suppression of the temperature ratio under different parameter conditions.

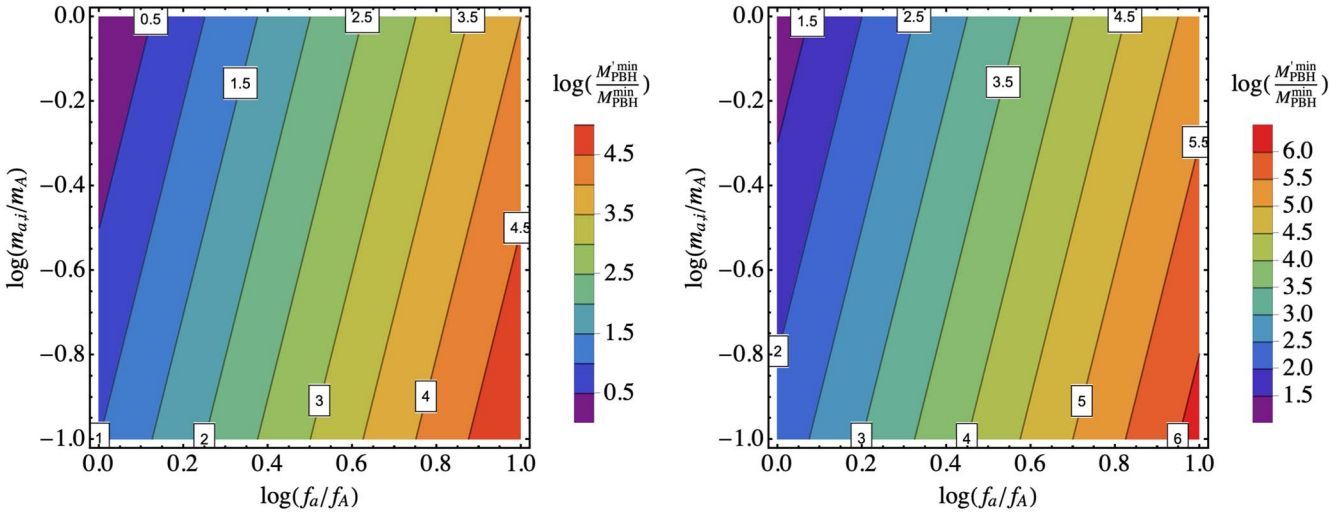

Figure 3. Variations in the minimum PBH mass ratio $M_{\rm PBH}^{'min}/M_{\rm PBH}^{\rm min}$, defined by equation (30), across the $\{\log(f_a/f_A), \log(m_{a,i}/m_A)\}$ parameter space. Left panel: we set $\theta_{i,A} = \pi$. Right panel: we set $\theta_{i,A} = \pi/2$. These panels not only demonstrate the variability in the minimum PBH mass ratio but also emphasize the potential for substantial mass enhancement under specific parameter configurations.

the minimum PBH mass can be enhanced by a factor

$$\frac{M_{\rm PBH}^{'min}}{M_{\rm PBH}^{\rm min}} \simeq \frac{\pi^4 m_A f_a^4}{m_{a,i} f_A^4 \theta_{i,A}^4}. \tag{30}$$

Figure 3 illustrates the distributions of this enhancement factor across the $\{\log(f_a/f_A), \log(m_{a,i}/m_A)\}$ plane, with $\theta_{i,A}$ fixed at π and $\pi/2$. Notably, these mass-enhanced PBHs could potentially serve as the seeds for supermassive black holes (SMBHs) at high redshifts [52].

Additionally, another intriguing phenomenon associated with the formation of QCD axion bubbles is the creation of axion miniclusters [24]. These miniclusters are gravitationally bound aggregations of axion DM [53–58]. The mass and size of these miniclusters are contingent upon the Hubble volume at the time when the QCD axion begins to oscillate. It is noteworthy that axion miniclusters can form when the bubbles enter the horizon prior to the axions becoming the dominant component of radiation within the bubbles. This condition sets the stage for the gravitational binding of axions, leading to the emergence of these miniclusters.

4. Conclusion

In summary, our investigation has focused on the modified formation of QCD axion bubbles in the context of resonant conversion between ALP and QCD axion. The formation of these bubbles can be attributed to an explicit breaking of the

PQ symmetry in the early Universe. We have introduced a generalized scenario where the QCD axion can mix with ALP prior to the QCD phase transition. Within this framework, resonant conversion from ALP to QCD axion is considered to occur at a temperature T_R, with the ALP energy density being adiabatic transferred to the QCD axion under specific conditions. Our findings reveal that this resonant conversion process leads to a suppression of the cosmic background temperature T_B at which the QCD axion energy density equals the radiation energy density. Subsequently, during the QCD phase transition, the emergence of QCD axions triggers the formation of axion bubbles. Furthermore, we have discussed the implications of this scenario for the formation of PBHs. Our analysis suggests that the minimum PBH mass can be increased to a certain extent, and these PBHs may potentially serve as the seeds for SMBHs.

Acknowledgments

The author would like to thank Wei Chao, Naoya Kitajima, Shota Nakagawa, Fuminobu Takahashi, and Yu-Feng Zhou for helpful discussions and valuable comments. This work was partly supported by the National Natural Science Foundation of China (NSFC) (Grants No. 11775025 and No. 12175027), and partly supported by the Key Laboratory of Theoretical Physics in the Institute of Theoretical Physics, CAS.

ORCID iDs

Hai-Jun Li https://orcid.org/0000-0001-9057-7898

References

[1] Peccei R D and Quinn H R 1977a CP conservation in the presence of instantons *Phys. Rev. Lett.* **38** 1440–3
[2] Peccei R D and Quinn H R 1977b Constraints imposed by CP conservation in the presence of instantons *Phys. Rev.* D **16** 1791–7
[3] Weinberg S 1978 A new light boson? *Phys. Rev. Lett.* **40** 223–6
[4] Wilczek F 1978 Problem of strong P and T invariance in the presence of instantons *Phys. Rev. Lett.* **40** 279–82
[5] 't Hooft G 1976 Symmetry breaking through Bell–Jackiw anomalies *Phys. Rev. Lett.* **37** 8–11
[6] 't Hooft G 1976 Computation of the quantum effects due to a four-dimensional pseudoparticle *Phys. Rev.* D **14** 3432–50
1978 *Erratum: Phys. Rev.* D **18** 2199
[7] Preskill J, Wise M B and Wilczek F 1983 Cosmology of the invisible axion *Phys. Lett.* B **120** 127–32
[8] Abbott L F and Sikivie P 1983 A cosmological bound on the invisible axion *Phys. Lett.* B **120** 133–6
[9] Dine M and Fischler W 1983 The not so harmless axion *Phys. Lett.* B **120** 137–41
[10] Di Luzio L, Giannotti M, Nardi E and Visinelli L 2020 The landscape of QCD axion models *Phys. Rept.* **870** 1–117
[11] Chadha-Day F, Ellis J and Marsh D J E 2022 Axion dark matter: what is it and why now? *Sci. Adv.* **8** abj3618
[12] Adams C B *et al* 2022 Axion dark matter arXiv:2203.14923
[13] Dine M and Anisimov A 2005 Is there a Peccei–Quinn phase transition? *J. Cosmol. Astropart. Phys.* **07** 009
[14] Jeong K S and Takahashi F 2013 Suppressing isocurvature perturbations of QCD axion dark matter *Phys. Lett.* B **727** 448–51
[15] Takahashi F and Yamada M 2015 Strongly broken Peccei-Quinn symmetry in the early Universe *J. Cosmol. Astropart. Phys.* 010
[16] Harigaya K, Ibe M, Schmitz K and Yanagida T T 2015 Peccei–Quinn symmetry from dynamical supersymmetry breaking *Phys. Rev.* D **92** 075003
[17] Kallosh R, Linde A D, Linde D A and Susskind L 1995 Gravity and global symmetries *Phys. Rev.* D **52** 912–35
[18] Banks T and Seiberg N 2011 Symmetries and strings in field theory and gravity *Phys. Rev.* D **83** 084019
[19] Witten E 2018 Symmetry and emergence *Nature Phys.* **14** 116–9
[20] Lee H-S and Yin W 2019 Peccei–Quinn symmetry from a hidden gauge group structure *Phys. Rev.* D **99** 015041
[21] Harlow D and Ooguri H 2019 Constraints on symmetries from holography *Phys. Rev. Lett.* **122** 191601
[22] Yin W 2020 Scale and quality of Peccei–Quinn symmetry and weak gravity conjectures *J. High Energy Phys.* JHEP10 (2020)032
[23] Jeong K S, Matsukawa K, Nakagawa S and Takahashi F 2022 Cosmological effects of Peccei–Quinn symmetry breaking on QCD axion dark matter *J. Cosmol. Astropart. Phys.* 026
[24] Kitajima N and Takahashi F 2020 Primordial black holes from QCD axion bubbles *J. Cosmol. Astropart. Phys.* 060
[25] Dolgov A D, Kawasaki M and Kevlishvili N 2009 Inhomogeneous baryogenesis, cosmic antimatter, and dark matter *Nucl. Phys.* B **807** 229–50
[26] Hasegawa F and Kawasaki M 2019 Primordial black holes from Affleck–Dine mechanism *J. Cosmol. Astropart. Phys.* 027
[27] Borsanyi S *et al* 2016 Calculation of the axion mass based on high-temperature lattice quantum chromodynamics *Nature* **539** 69–71
[28] di Cortona G G, Hardy E, Vega J P and Villadoro G 2016 The QCD axion, precisely *J. High Energy Phys.* JHEP01 (2016)034
[29] Turner M S 1986 Cosmic and local mass density of invisible axions *Phys. Rev.* D **33** 889–96
[30] Lyth D H 1992 Axions and inflation: sitting in the vacuum *Phys. Rev.* D **45** 3394–404
[31] Visinelli L and Gondolo P 2009 Dark matter axions revisited *Phys. Rev.* D **80** 035024
[32] Aghanim N *et al* 2020 Planck 2018 results. VI. cosmological parameters *Astron. Astrophys.* **641** A6
2021 *Erratum: Astron. Astrophys.* **652** C4
[33] Nomura Y, Rajendran S and Sanches F 2016 Axion isocurvature and magnetic monopoles *Phys. Rev. Lett.* **116** 141803
[34] Kawasaki M, Takahashi F and Yamada M 2016 Suppressing the QCD axion abundance by hidden monopoles *Phys. Lett.* B **753** 677–81
[35] Kawasaki M, Takahashi F and Yamada M 2018 Adiabatic suppression of the axion abundance and isocurvature due to coupling to hidden monopoles *J. High Energy Phys.* JHEP01(2018)053
[36] Chiba T, Takahashi F and Yamaguchi M 2004 Baryogenesis in a flat direction with neither baryon nor lepton charge *Phys. Rev. Lett.* **92** 011301
2015 *Erratum: Phys. Rev. Lett.* **114** 209901
[37] Takahashi F and Yamaguchi M 2004 Spontaneous baryogenesis in flat directions *Phys. Rev.* D **69** 083506

[38] Higaki T, Jeong K S and Takahashi F 2014 Solving the tension between high-scale inflation and axion isocurvature perturbations *Phys. Lett.* B **734** 21–6
[39] Co R T, Hall L J and Harigaya K 2020 Axion kinetic misalignment mechanism *Phys. Rev. Lett.* **124** 251802
[40] Choi K, Kim H B and Kim J E 1997 Axion cosmology with a stronger QCD in the early Universe *Nucl. Phys.* B **490** 349–64
[41] Ho S-Y, Saikawa K and Takahashi F 2018 Enhanced photon coupling of ALP dark matter adiabatically converted from the QCD axion *J. Cosmol. Astropart. Phys.* 042
[42] Li H-J 2024 Axion dark matter with explicit Peccei–Quinn symmetry breaking in the axiverse *J. Cosmol. Astropart. Phys.* 025
[43] Bird S, Cholis I, Muñoz J B, Ali-Haïmoud Y, Kamionkowski M, Kovetz E D, Raccanelli A and Riess A G 2016 Did LIGO detect dark matter? *Phys. Rev. Lett.* **116** 201301
[44] Carr B and Kuhnel F 2020 Primordial black holes as dark matter: recent developments *Ann. Rev. Nucl. Part. Sci.* **70** 355–94
[45] Green A M and Kavanagh B J 2021 Primordial black holes as a dark matter candidate *J. Phys.* G **48** 043001
[46] Carr B and Kuhnel F 2022 Primordial black holes as dark matter candidates *SciPost Phys. Lect. Notes* 1 **48**
[47] Li H-J 2022 Primordial black holes induced stochastic axion-photon oscillations in primordial magnetic field *J. Cosmol. Astropart. Phys.* 045
[48] Carr B J, Kohri K, Sendouda Y and Yokoyama J 2010 New cosmological constraints on primordial black holes *Phys. Rev.* D **81** 104019
[49] Carr B J 1975 The primordial black hole mass spectrum *Astrophys. J.* **201** 1–19
[50] Kopp M, Hofmann S and Weller J 2011 Separate universes do not constrain primordial black hole formation *Phys. Rev.* D **83** 124025
[51] Carr B J and Harada T 2015 Separate universe problem: 40 years on *Phys. Rev.* D **91** 084048
[52] Li H-J, Peng Y-Q, Chao W and Zhou Y-F 2024 Supermassive black holes triggered by QCD axion bubbles *Commun. Theor. Phys.* **76** 055405
[53] Hogan C J and Rees M J 1988 Axion miniclusters *Phys. Lett.* B **205** 228–30
[54] Kolb E W and Tkachev I I 1993 Axion miniclusters and Bose stars *Phys. Rev. Lett.* **71** 3051–4
[55] Fairbairn M, Marsh D J E, Quevillon J and Rozier S 2018 Structure formation and microlensing with axion miniclusters *Phys. Rev.* D **97** 083502
[56] Xiao H, Williams I and McQuinn M 2021 Simulations of axion minihalos *Phys. Rev.* D **104** 023515
[57] Ellis D, Marsh D J E, Eggemeier B, Niemeyer J, Redondo J and Dolag K 2022 Structure of axion miniclusters *Phys. Rev.* D **106** 103514
[58] Dandoy V, Schwetz T and Todarello E 2022 A self-consistent wave description of axion miniclusters and their survival in the galaxy *J. Cosmol. Astropart. Phys.* 081